Supplementary Materials

Wireless, Flexible, Ion-Selective Electrode System for Selective and Repeatable Detection of Sodium

Hyo-Ryoung Lim [1], Yun-Soung Kim [1], Shinjae Kwon [1], Musa Mahmood [1], Young-Tae Kwon [1], Yongkuk Lee [2], Soon Min Lee [3], and Woon-Hong Yeo [1,4,5,*]

1. George W. Woodruff School of Mechanical Engineering, Institute for Electronics and Nanotechnology, Georgia Institute of Technology, Atlanta, GA, 30332, USA; hlim308@gatech.edu (H-.R. L.); ysk@me.gatech.edu (Y-.S.K.); skwon64@gatech.edu (S.K.); musamahmood@gatech.edu (M.M.); ykwon87@gatech.edu (Y-.T.K.)
2. Department of Biomedical Engineering, Wichita State University, Wichita, KS 67260, USA; yongkuk.lee@wichita.edu
3. Department of Pediatrics, Gangnam Severance Hospital, Yonsei University College of Medicine, Seoul, South Korea; smlee@yuhs.ac
4. Wallace H. Coulter Department of Biomedical Engineering, Georgia Institute of Technology & Emory University School of Medicine, Atlanta, GA, 30322, USA
5. Parker H. Petit Institute for Bioengineering and Biosciences, Institute for Materials, Neural Engineering Center, Institute for Robotics and Intelligent Machines, Georgia Institute of Technology, Atlanta, GA, 30332, USA

* Correspondence: whyeo@gatech.edu (W-.H.Y.); Tel.: +1-404-385-5710; Fax: +1-404-894-1658

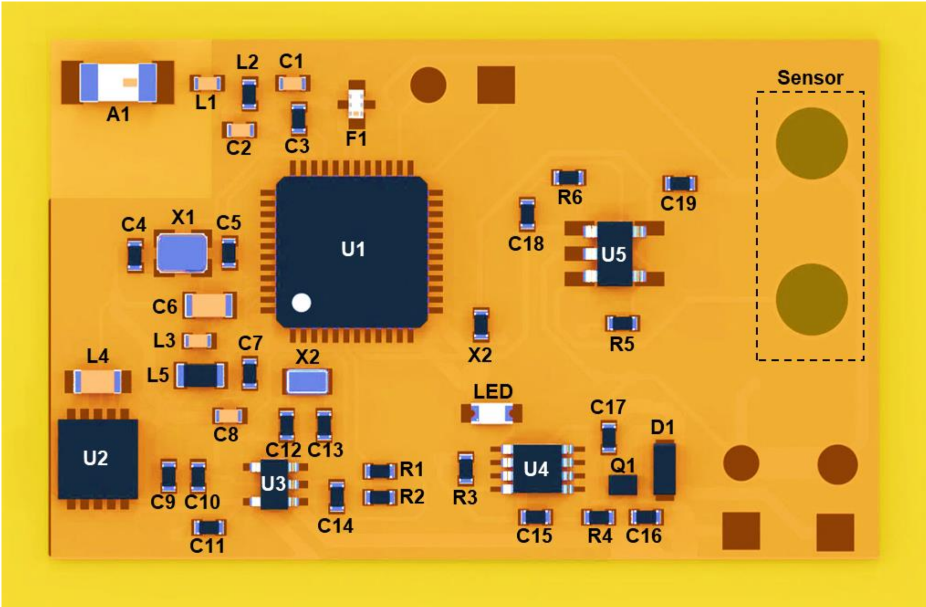

Figure S1. Illustration of wireless ion-selective sodium sensor circuit components with detail list of the surface mount chip components in Table S1. The sensor includes an ion-selective electrode (ISE) and an Ag/AgCl reference electrode (RE), which are directly formed onto Cu-pads of the circuit.

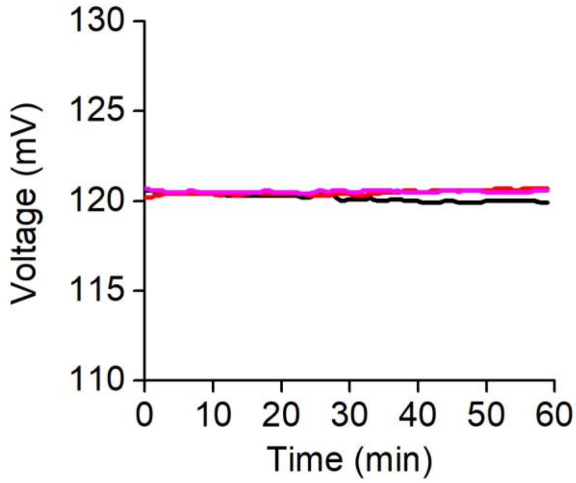

Figure S2. Voltage stability (0.53 mV/h; n = 3) of the all-solid-state film sodium ISE in 10^{-2} M sodium chloride.

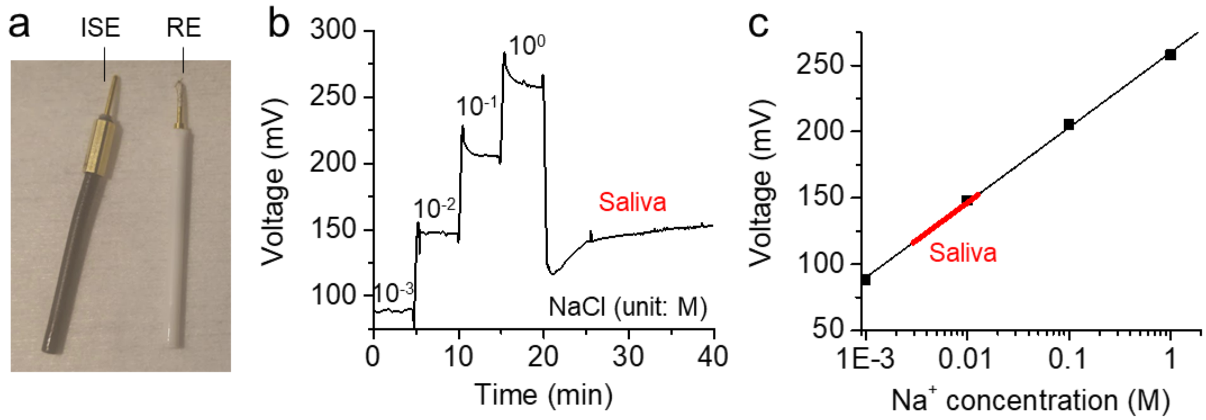

Figure S3. Saliva concentration measured with using a commercial all-solid-state ISE and RE. (a) Photograph of the commercial sodium ISE and RE. (b) Voltage response of the sensor in NaCl solutions and Saliva. (c) Saliva concentration shows 3-13 mM Na^{+} (highlighted in red on the calibration line with a slope of 56 mV/decade).

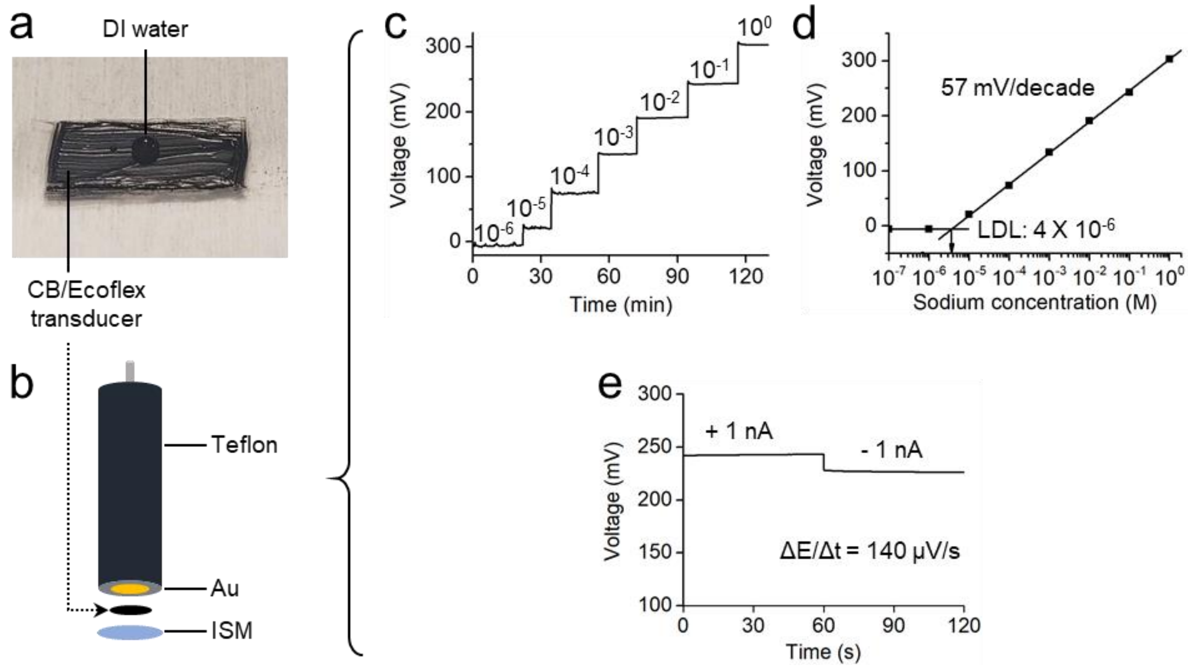

Figure S4. Sensing capabilities of a CB/Ecoflex-based ISE formed on a standard Teflon-body electroe. (a) Photograph showing a hydrophobicity of the CB/Ecoflex composite, ensuring a good contact with the PVC ISM. (b) Schematic diagram of the structure of CB/Ecoflex/ISM formed on an Au disc shrouded by Teflon. Sensing capabilities measured with using the ISE (b): (c) Real-time voltage response in 10^{-6} to 10^{0} sodium chloride solutions, (d) calculated sensitivity and low detection limit (LDL), and (e) voltage stability measured by chronopotentiometry in 10^{-2} sodium chloride.

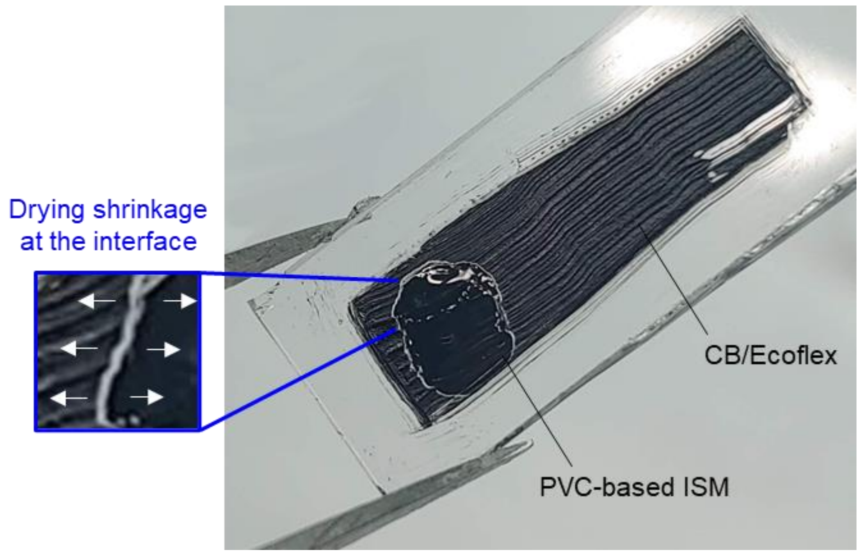

Figure S5. Photograph showing a drying shrinkage at the interface between a CB/Ecoflex transducer and ISM that contains THF, resulted in a delamination.

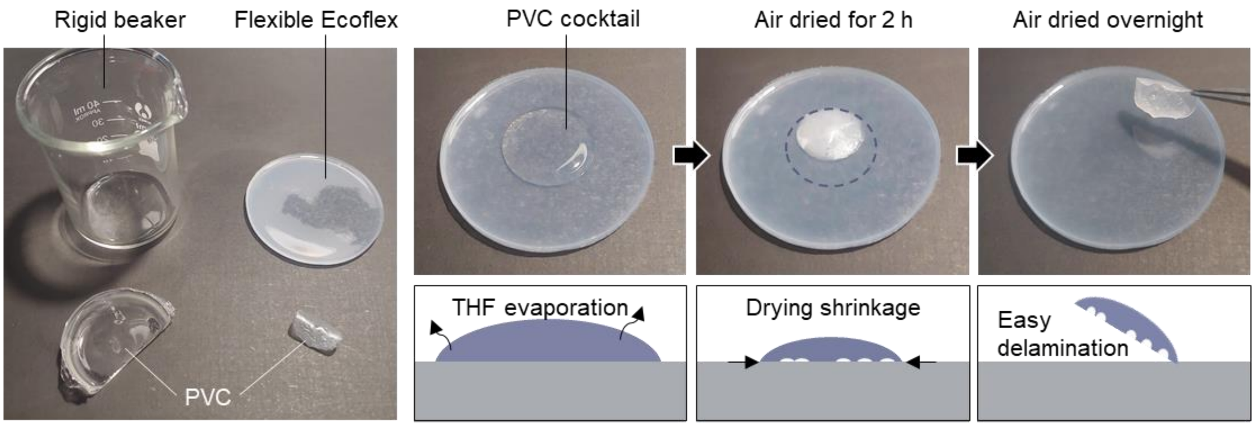

Figure S6. Photographs showing a drying shrinkage of PVC formed on the surface of Ecoflex compared to a rigid beaker. While the PVC cocktail in the beaker was dried stuck at the surface of the rigid glass, the film formed on the flexible substrate shows a significant shrinkage and pores.

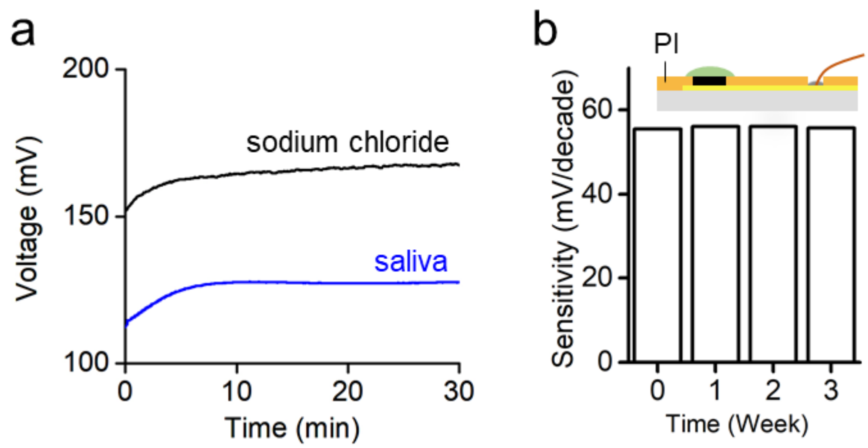

Figure S7. Short-term and long-term stable voltage reading of an all-solid-state film ISE enabled by efficient chemical insulation. (a) Voltage reading of the sensor in 10^{-1} sodium chloride solution and saliva. (b) Long-term stability of stability for three weeks.

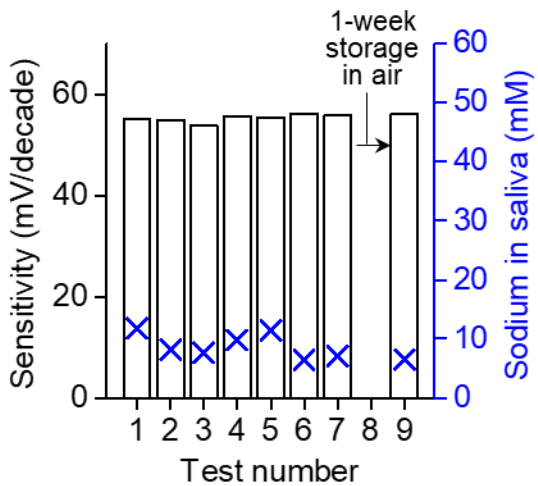

Figure S8. Sensitivity and applicability of sodium detection of our film ISE during 1-week storage in air. The 7 times measurement was conducted continuously.

Table S1. List of surface mount components used in wireless ion-selective sodium sensor circuit.

Component	Description	Value	Part number
U1	Bluetooth PSoC	N/A	NRF52832-QFAA-R
U2	3.3 voltage regulator	N/A	TPS63001
U3	Current limit active-low load switch	N/A	TPS22941
U4	Battery recharge	N/A	MCP73831
U5	Single channel Op-amp IC	N/A	AD8603AUJZREEL7
F1	2.45 GHz low pass filter	N/A	2450FM07A0029
A1	2.45 GHz RF chip antenna	N/A	2450AT18A100
D1	Schottky Diode	N/A	641-1285-1-ND
Q1	P-MOSFET	N/A	DMP21D5UFB4-7BDICT-ND
X1	32 MHz crystal	N/A	ECS-320-8-37CKM
X2	32.768 kHz crystal	N/A	ECS-327-9-12-TR
L1	0402 inductor	3.9 nH	N/A
L2	0402 inductor	2.7 nH	N/A
L3	0402 inductor	15 nH	N/A
L4	0603 inductor	2.2 μH	N/A
L5	0603 inductor	10 μH	N/A
C1	0402 ceramic capacitor	1.0 pF	N/A
C2, C8	0402 ceramic capacitor	100 nF	N/A
C3	0402 ceramic capacitor	100 pF	N/A
C4, C5, C12, C13	0402 ceramic capacitor	12 pF	N/A
C6	0603 ceramic capacitor	1.0 μF	N/A
C7, C15, C17	0402 ceramic capacitor	4.7 μF	N/A
C9	0402 ceramic capacitor	22 μF	N/A
C10, C11, C14, C18	0402 ceramic capacitor	10 μF	N/A
C16	0402 ceramic capacitor	1.0 μF	N/A
C19	0402 ceramic capacitor	10 nF	N/A
R1, R2	0402 resistor	1 MΩ	N/A
R3	0402 resistor	2 kΩ	N/A
R4	0402 resistor	100 kΩ	N/A
R5, R6	0402 resistor	10 kΩ	N/A
Battery	Lithium-ion polymer		

Table S2. Comparison of sensing capabilities based on carbon-polymer composite transducers.

Year[Reference]	**Transducer**	**Sensitivity mV/decade)**	**Range (M)**	**Ion**
This work[2020]	Carbon black/Ecoflex	57.0	10^{-6} to 1	Na^+
[1][2009]	CNT/block polymer	58.6	10^{-7} to 10^{-1}	Na^+
[2][2010]	CNT/block polymer/ISM	58.2	10^{-6} to 10^{-1}	Na^+
[3][2019]	CNT/copolymer	56.3	10^{-7} to 10^{-1}	K^+
[4][2017]	CNT/porphyrinoids	60.5	10^{-7} to 10^{-1}	K^+
[5][2015]	Graphene/AgTFPB	56.5	10^{-5} to 10^{-2}	K^+

References

1. Zhu, J.; Qin, Y.; Zhang, Y., Preparation of all solid-state potentiometric ion sensors with polymer-CNT composites. *Electrochemistry Communications* **2009,** 11, (8), 1684-1687.
2. Zhu, J.; Li, X.; Qin, Y.; Zhang, Y., Single-piece solid-contact ion-selective electrodes with polymer–carbon nanotube composites. *Sensors and Actuators B: Chemical* **2010,** 148, (1), 166-172.
3. Kałuża, D.; Jaworska, E.; Mazur, M.; Maksymiuk, K.; Michalska, A., Multiwalled Carbon Nanotubes–Poly(3-octylthiophene-2,5-diyl) Nanocomposite Transducer for Ion-Selective Electrodes: Raman Spectroscopy Insight into the Transducer/Membrane Interface. *Analytical Chemistry* **2019,** 91, (14), 9010-9017.
4. Jaworska, E.; Naitana, M. L.; Stelmach, E.; Pomarico, G.; Wojciechowski, M.; Bulska, E.; Maksymiuk, K.; Paolesse, R.; Michalska, A., Introducing Cobalt(II) Porphyrin/Cobalt(III) Corrole Containing Transducers for Improved Potential Reproducibility and Performance of All-Solid-State Ion-Selective Electrodes. *Analytical Chemistry* **2017,** 89, (13), 7107-7114.
5. Sun, Q.; Li, W.; Su, B., Highly hydrophobic solid contact based on graphene-hybrid nanocomposites for all solid state potentiometric sensors with well-formulated phase boundary potentials. *Journal of Electroanalytical Chemistry* **2015,** 740, 21-27.